nature nanotechnology

ARTICLES

PUBLISHED ONLINE: 15 AUGUST 2016 | DOI: 10.1038/NNANO.2016.153

Direct observation of DNA knots using a solid-state nanopore

Calin Plesa[1], Daniel Verschueren[1], Sergii Pud[1], Jaco van der Torre[1], Justus W. Ruitenberg[1], Menno J. Witteveen[1], Magnus P. Jonsson[1†], Alexander Y. Grosberg[2], Yitzhak Rabin[3] and Cees Dekker[1*]

Long DNA molecules can self-entangle into knots. Experimental techniques for observing such DNA knots (primarily gel electrophoresis) are limited to bulk methods and circular molecules below 10 kilobase pairs in length. Here, we show that solid-state nanopores can be used to directly observe individual knots in both linear and circular single DNA molecules of arbitrary length. The DNA knots are observed as short spikes in the nanopore current traces of the traversing DNA molecules and their detection is dependent on a sufficiently high measurement resolution, which can be achieved using high-concentration LiCl buffers. We study the percentage of molecules with knots for DNA molecules of up to 166 kilobase pairs in length and find that the knotting occurrence rises with the length of the DNA molecule, consistent with a constant knotting probability per unit length. Our experimental data compare favourably with previous simulation-based predictions for long polymers. From the translocation time of the knot through the nanopore, we estimate that the majority of the DNA knots are tight, with remarkably small sizes below 100 nm. In the case of linear molecules, we also observe that knots are able to slide out on application of high driving forces (voltage).

It is well established that long polymers are subject to increasing self-entanglement as their length increases. DNA knots have been the focus of significant study in polymer physics[1,2] and although they are ubiquitous in nature[3], their exact role in biological processes is still under investigation[4–6]. Despite this interest, knotting remains among the least understood properties of polymers due to a lack of both experimental techniques for observing them as well as rigorous theoretical approaches to describing and characterizing them. Many open questions remain[7], such as what determines the characteristic chain length beyond which knots become prevalent on cyclization, knot localization[8,9], the existence of metastable tight knots[10], among others.

A number of experimental techniques have been developed to study knots, particularly in DNA. Knots have been induced with high electric fields[11], optical tweezers[12,13], topoisomerase enzymes[14–16], DNA recombinases[17] and through the cyclization of linear DNA molecules[18,19]. Electron microscopy[14] and atomic force microscopy[20] have been used to image knots with excellent resolution but these techniques are limited to small molecules and low statistics. Optical techniques[11,12] have been used to introduce knots and study their behaviour in DNA strands. Gel electrophoresis[15,16,18,19,21], the dominant tool used in knot studies, is a bulk technique where knots are trapped in circular molecules that are limited to lengths in the range of 10 kilobase pairs (kbp) or lower.

Solid-state nanopores have emerged as an important tool with a large number of potential applications[22,23] at the crossroads of physics, biology and chemistry. Nanopores have provided a method for investigating various concepts in polymer physics such as polymer translocation through pores[24,25], the Zimm relaxation time[25,26] and the polymer capture process[27,28]. In nanopore sensing, biomolecules in an aqueous solution are placed into one of two reservoirs that are separated by a 20 nm-thick membrane containing a nanometre-scale pore (Fig. 1). The subsequent application of a voltage using electrodes bathed in each reservoir produces an electric field and a resulting electrophoretic force on charged molecules such as DNA, causing them to be pulled through the nanopore. The presence of a molecule in the pore causes a blockade in the ionic current that (in high-salinity conditions) is proportional to the volume of the segment of the molecule in the pore. For long polymers, the translocation process is much faster than the typical relaxation time[29], which allows us to investigate the polymers before they have a chance to relax. This enables us to probe long DNA molecules for the presence of topological structures such as knots. Several theoretical papers have addressed some of the issues arising from the presence of knots in molecules translocating through nanopores[30–33]. Here we report the direct experimental observation of knots in measurements on long double-stranded DNA (dsDNA) molecules that translocate through solid-state nanopores.

Ionic current signatures of DNA knots

Knots produce distinctive signatures in the current blockade of translocating DNA molecules. When a linear unknotted DNA molecule passes through the pore, it causes a blockade with magnitude I_1 in the current level as shown in Fig. 2a. If the molecule enters the pore in a folded configuration this produces a blockade level that is twice as high ($2I_1$) for the duration of the fold, as shown in Fig. 2b. These folds occur primarily at the start of the translocation process and their probability of occurrence has been shown to increase as the capture point gets closer to the end of the molecule[28]. High-resolution investigation of DNA translocation events reveals the presence of further sharp blockage spikes with a high amplitude and very short duration occurring within a fraction of the events. Examples of such events are shown in Fig. 2c,d,f. We observe such events in both linear DNA (Fig. 2c,d) and circular dsDNA

[1]Department of Bionanoscience, Kavli Institute of Nanoscience, Delft University of Technology, Van der Maasweg 9, 2629 HZ Delft, The Netherlands. [2]Department of Physics and Center for Soft Matter Research, New York University, 4 Washington Place, New York, New York 10003, USA. [3]Department of Physics and Institute for Nanotechnology and Advanced Materials, Bar Ilan University, Ramat Gan 52900, Israel. †Present address: Department of Science and Technology, Campus Norrköping, Linköping University, SE-60174 Norrköping, Sweden. *e-mail: c.dekker@tudelft.nl

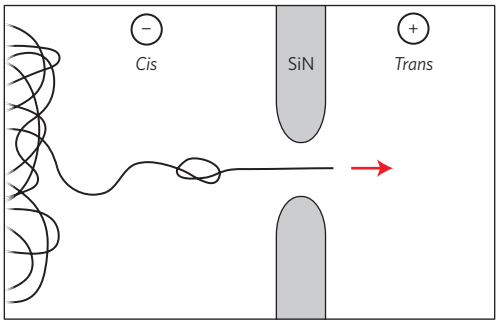

Figure 1 | A schematic illustration of a DNA molecule with a knot translocating through a solid-state nanopore. A trefoil (3_1) knot is shown in a simplified diagram of the process; in reality, the knot may be located anywhere within the DNA blob, and most of the strands of the blob will be closer to the nanopore opening.

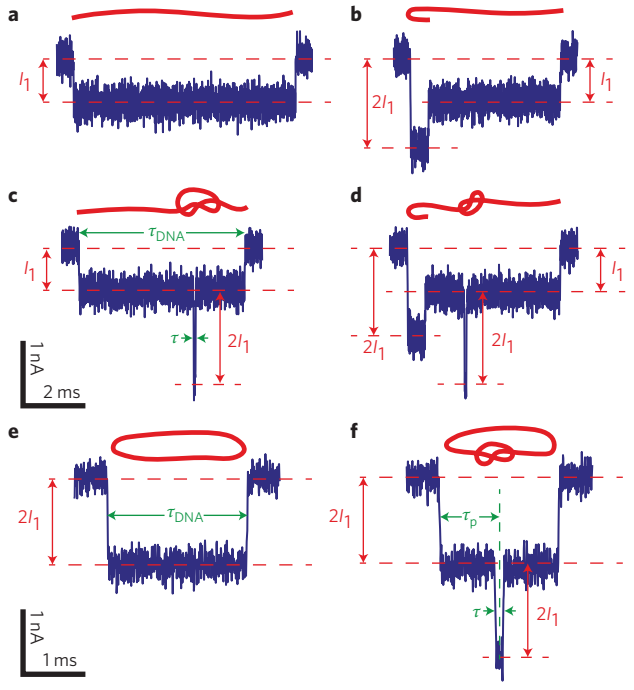

Figure 2 | Six example events for lambda DNA translocating through a 10 nm pore at 200 mV in 2 M LiCl at 30 kHz bandwidth. The molecular configuration attributed to each type of event is shown above each current trace in red. **a**, Current trace of an unfolded event. **b**, Current trace of an event with a fold at the start. **c**, Current trace of an event with an internal blockade, which can be associated with a knot. The blockade has an additional amplitude of $2I_1$ on top of the I_1 blockade from the linear molecule, consistent with a total of 3 dsDNA strands that occupy the pore at the moment that the knot is translocating. **d**, Another event similar to **c** but with an additional fold at the start. **e**, Current trace of an unfolded circular molecule translocating. **f**, Current trace of a circular molecule containing a knot. The blockade has an additional amplitude of $2I_1$ on top of the $2I_1$ blockade from the circular molecule, consistent with a total of 4 dsDNA strands in the pore while the knot is translocating.

(Fig. 2f and Supplementary Fig. 18c,d). These spikes occur only within the DNA translocation events and have an amplitude (on top of the DNA blockade level I_1) that is an integer multiple of $2I_1$. Such spikes can only be associated with two types of molecular configurations: an internal fold within the molecule (Supplementary Fig. 5ii), or a topologically constrained DNA knot (Supplementary Fig. 5i). The former configuration of local folds has extremely low rates of occurrence due to the nature of the translocation process, which can be seen as follows. The nanopore can be thought of as applying a point force to the polymer at the location of the nanopore, as the electric field strength is highest in the pore and strongly decreases by $1/r^2$ away from the pore[34]. A long DNA molecule coils up into a polymer blob that has a large size (many hundreds of nanometres) compared with the nanometre-size nanopore. For translocation, a DNA end is pulled though the pore, thus disentangling the blob. The tension in the DNA strand that results from the pulling action towards the pore propagates along the strand outwards from the nanopore, which pulls out any internal folds (because the velocity of the leading (captured) DNA is much higher than that of the lagging DNA (behind the fold)). Knots, on the other hand, cannot unfold due to the topological constraints imposed and are pulled towards and translocated through the nanopore. This argument that the observed blockades are due to knots as opposed to folds is strongly supported by the small size observed for the majority of knots, the higher-order ($4I_1$, $6I_1$ and so on) current blockades observed, the observation of knot sliding and the differences in occurrence observed between linear and circular molecules. A detailed overview of all of the arguments supporting this conclusion can be found in Supplementary Section 2.

The observed current signatures allow us to probe the knotting probability, knot size and knot position. The $2I_1$ additional magnitude of the spikes provides strong evidence for the occurrence of DNA knots, indicating the presence of three dsDNA segments in total within the nanopore. Although the knot amplitude can be used to determine the number of dsDNA strands inside the pore, the current signatures for the knots do not provide information about the crossing number of the knot. Different knot types (trefoil, figure-eight and so on) have the same number of dsDNA strands when linearly stretched out (without changing the topology of the knot) and accordingly can have the same number of dsDNA strands simultaneously inside the pore during translocation. As a consequence, our experimental results lead to statements encompassing many knot types. Most spikes that we observe consistently have an amplitude of $2I_1$ beyond the normal DNA blockage level. Occasionally, however, we observe events during which the additional current blockade has an amplitude of only I_1 (beyond the normal DNA blockage level), which may be due to the presence of replication forks (which occur due to the nature of the plasmid replication process) or due to simultaneous co-translocation of two different molecules. This latter phenomenon is only significant if either a high concentration of DNA is used or if there is a significant number of smaller DNA fragments due to handling, and such events can easily be distinguished from the blockades produced by knots (Supplementary Section 2). For circular DNA molecules, DNA catenanes may be possible as well. Higher-order blockades ($4I_1$, $6I_1$, $8I_1$ and so on), as shown in Supplementary Fig. 18, are observed in a small fraction of events and can be attributed to more complex knots, because these higher-order knot structures each bring two additional dsDNA strands simultaneously into the pore. The fraction of these complex knots increases as a function of increasing polymer length[33,35].

In common nanopore experiments knots are hard to observe as their small size (<100 nm; see below) makes their observation very sensitive to the resolution of the solid-state nanopore measurement. Most nanopore experiments are carried out in 1 M KCl[25–28], in which most observed knots have a duration (τ) of 15 μs at 100 mV, indicating that their detection is at the edge of what is resolvable (Supplementary Section 4). For this reason the majority of the experiments presented in this study are carried out in solutions of 2 M or 4 M LiCl, which (as we have previously shown) can increase the translocation time of DNA by a factor of 7 or 10, respectively, relative to 1 M KCl[36]. Furthermore, the conductance blockades are also higher in 2 M and 4 M LiCl, which leads to a higher

signal-to-noise-ratio (SNR) and allows for higher measurement bandwidths. Indeed, for 48.5 kbp DNA molecules under the same conditions, we observe fewer than 50% of the knots in 1 M KCl relative to measurements in a 2 M LiCl solution, as discussed below.

Knotting probability as a function of DNA length

We measured molecules of different lengths to study how the knotting probability scales as a function of DNA length, and we compare the observed rates of knot occurrence with previous simulation-based predictions. Four different DNA lengths were used: 2,686 bp pUC19 linearized with XmnI, a 20,678 bp linearized plasmid, 48,502 bp lambda phage DNA and 165,648 bp phage T4 GT7 DNA. Figure 3 shows the measured knotting probabilities and their standard deviations for linear molecules as a function of DNA molecule length (Supplementary Section 1). The observed scaling can be fitted with a simple model, described below, which is linear below approximately 40 kbp. For 2,686 bp molecules in 4 M LiCl we find a knotting probability of 1.8%, whereas for the 20,678 bp molecules we observe 13.8 ± 1.0% of molecules to have knots. For 48,502 bp molecules we find 26.8 ± 3.4% of molecules contain knots, while similar measurements carried out in 2 M LiCl find a 24.4 ± 4.6% knotting occurrence (Supplementary Section 8). As these molecules are linear, the knotting probabilities may be reduced due to the effect of knots slipping out, as discussed in detail below. We fit the observed scaling of the knotting occurrence with length using a model of the form $P = 1-\exp(-N/N_0)$, where N is the length in bp, and N_0 is the random knotting length (details in Supplementary Section 3). We find a fitted value of 143 ± 5 kbp for N_0. As mentioned above, data taken in 1 M KCl showed significantly lower knotting levels, an effect that is attributed to the limited resolution of these measurements. Nevertheless, it can provide a lower bound for the knot probability. These results provide the first experimental validation of the knotting abundances in long polymers.

The observed rates of knotting occurrence are co-plotted in Fig. 3 alongside simulation-based predictions[18,35] (Supplementary Section 9). These simulated rates do not include complex knots and thus can only serve as a lower bound as the number of more complex knots increases significantly as a function of the polymer length. For 2,686, 20,678, 48,502 and 165,648 bp DNA molecules these simulations predict knotting rates of 0.2, 14, 35 and 80% respectively. Qualitatively we thus clearly see that the simulation-based predictions show the same overall trend as the experiments. Because our measurements are carried out in very high ionic strength conditions where the electrostatic screening is very strong, we expect the effective diameter to be very close to the physical diameter of DNA. This leads to higher knotting probabilities relative to those expected in the case of lower ionic strength regimes, such as those found at physiological conditions[18].

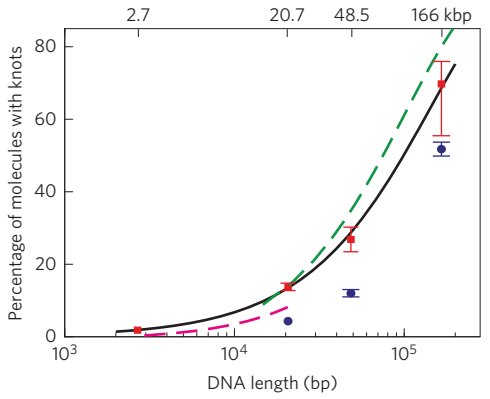

Figure 3 | Percentage of events with knots as a function of DNA length. Measurements were carried out in 4 M LiCl (red squares) and 1 M KCl (blue circles) for linear dsDNA molecules in 20 nm pores. Error bars indicate the standard deviation, except for the data point for 166 kbp in 4 M LiCl (Supplementary Section 3). The 1 M KCl data provide a lower limit of the knot occurrence due to the low resolution. The dashed lines represent knot occurrence predictions based on simulations in ref. 35 (green) and ref. 18 (magenta) (Supplementary Section 9). The solid line is a fit of $1-\exp(-N/N_0)$ viewing localized knots as a Poisson process, with $N_0 = 143 \pm 5$ kbp (Supplementary Section 3).

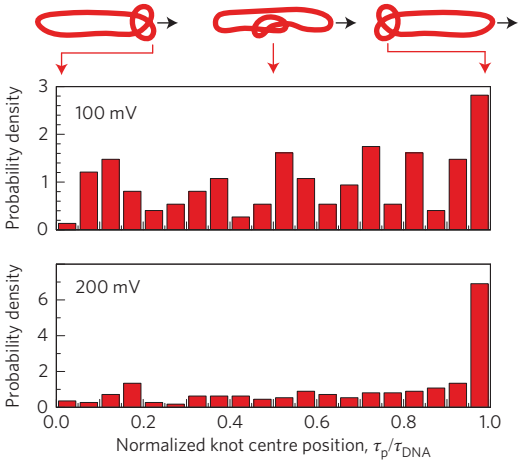

Figure 4 | Normalized centre position of knots observed in 20.7 kbp relaxed circular molecules. The experiments were performed in 4 M LiCl at 100 mV (top) and 200 mV (bottom). $\tau_p/\tau_{DNA} = 0$ denotes the start of the translocation and $\tau_p/\tau_{DNA} = 1$ the end of the translocation event. As the voltage is increased, we see knots sliding towards the end of the molecule.

DNA knot position, sliding and slipping out

As these measurements are carried out on linear molecules, we investigated the possibility of knots slipping out before being captured. Once a knot reaches the pore, translocation can only occur after the knotted strand has been bent to a size set by the pore diameter, that is, on scales below the persistence length of dsDNA. If this process does not occur quickly enough, the low-friction DNA–DNA interactions could allow a knot to slip out[12,30,37] by remaining at the pore entrance while the non-knotted DNA strand translocates through (Supplementary Fig. 6a). In circular DNA molecules, however, the closed curve topology prevents such slipping out and knots are intrinsically trapped. We investigated the position of the observed knots in 20.7 kbp relaxed circular molecules where any knots contained inside would not be able to escape, although within a translocation event they might slip until the end. Figure 4 shows the normalized centre position of the knots (τ_p/τ_{DNA}) in a 20 nm pore in 4 M LiCl for applied voltages of 100 and 200 mV. We observe that knots occur at random positions for 100 mV, whereas at 200 mV they indeed occur with a strong preference for the end of the molecule that translocates through the pore last. We thus see a clear indication that the higher voltage causes knots to slide towards the end of the molecule. As a consequence, the numbers for the knot occurrence in linear molecules (Fig. 3) provide a reasonable value at a low applied voltage (100 mV), but should be treated as a lower bound to the equilibrium knotting levels at higher voltages, where a significant number of the knots may slip out. To quantify the number of knots that slip out, we carried out experiments using lambda phage DNA (48.5 kbp). This molecule has a 12 bp complementary overhang, allowing it to exist in both linear and circular forms depending on the temperature and salinity conditions[38]. We heated solutions of lambda

DNA and quickly cooled them while in 2 M LiCl, to form mixed populations of linear and circular DNA from which to compare the knotting occurrence. No temperature dependence for the knotting probability was observed in a previous study[18], allowing us to attribute any differences between the knotting occurrence in the two populations to knots slipping out. We observed a 55% higher knotting occurrence in the circular molecules compared with the linear ones (Supplementary Section 8). Furthermore, we have tentative evidence that suggests knot sliding can sometimes be directly observed within the current trace of a translocation event, as shown in Supplementary Fig. 19. This effect is due to a slight increase in the current blockade caused by the knot sitting against the pore mouth before being translocated, and is consistent with similar effects reported in the literature for DNA docked onto the pore mouth[39–41]. These results indicate that knots are able to slip out of linear DNA molecules during their translocation through nanopores.

DNA knot size

We estimated the sizes of the knots from the time required for the knots to translocate through the nanopore. This estimate uses the average velocity of the DNA translocation, which is determined by dividing the known length of the molecules by their total translocation time. The total contour length of the DNA within the knot can be determined by multiplying the knot size by the total number of strands in the knot (which is three for simple knots such as trefoil, figure-eight and so on). Figure 5 shows the measured time duration of knots on a log scale for linear 20.7 kbp molecules at 100 mV. The vertical dashed line indicates the filtering distortion point, which is twice the rise time of the filter ($2T_r$), while the solid line is a fit to the model described below. We estimate the sizes of the knots to be in the tens of nanometres at both 100 and 200 mV (Supplementary Section 6), assuming mean translocation velocities (Supplementary Section 7) of 872 and 1,937 nm ms^{-1} respectively, as shown on the top x axis of Fig. 5. Note that such a small knot size indicates that the DNA knots in these long DNA polymers are remarkably tight. The numbers may underestimate the size of the knots somewhat, especially for those that occur at the end of the translocation process where we know that the velocity is higher than average[42,43]. Measurements on circular versions of the same molecules under the same conditions reveal similar distributions of very tight knots (Supplementary Section 6). From all of our data, we conclude that the majority of DNA knots have a size below 100 nm. The observation of these tight knots provides evidence for the occurrence of metastable tight knots that have been predicted to exist at equilibrium in long polymers[10,44]. Given the nature of the translocation process, it remains to be determined how much these knots are being tightened relative to their equilibrium sizes, although the similar numbers for the data at 100 versus 200 mV and linear versus circular DNA suggest that the tight knots are intrinsic.

The knot translocation duration distribution $P(\tau)$ is consistent with a model based on the previously proposed[10] free-energy penalty for knot formation, that is, $P(\tau) = A\exp(-(c_1/\tau) - c_2\tau^{1/3})$, where A is the normalization factor and the two terms in the exponential reflect the bending energy and confinement entropy contributions, respectively. Although this distribution was originally derived for the knot length and knot size, we adopt it here to characterize the knot translocation duration, which is assumed to scale linearly with knot size. Fits were made to the data for 20,678 bp DNA in 4 M LiCl at 100 mV in 20 nm pores, see Fig. 5. This yields $c_2 = 0.61 \pm 0.09\ \mu s^{-1/3}$, although it is hard to obtain reliable estimates for c_1, as the fitted values range from 0.3 to 18 μs. Physically, coefficient c_1 controls the decay of probability for very small τ, (that is, for very tight knots) and the large uncertainty in its magnitude is due to knots slipping out as well as the limited temporal resolution of the measurements[45]. The tail of the distribution is consistent with the functional form $\exp(-c_2\tau^{1/3})$, which theoretically derives from DNA undulations inside the effective tube formed by the knot.

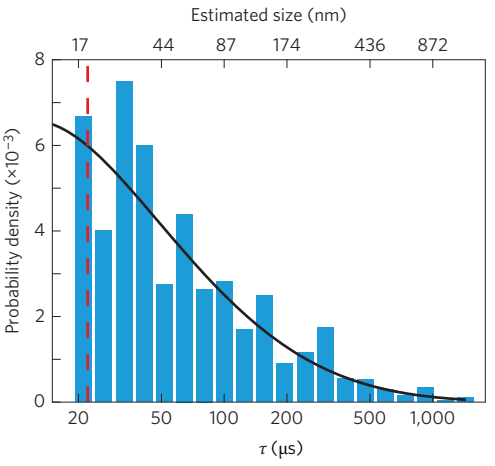

Figure 5 | Translocation duration of knots (τ) observed in 20.7 kbp linear molecules in 4 M LiCl at 100 mV. Note the logarithmic timescale. The black line is a fit to the model described in the main text, while the dashed red line indicates the filtering distortion point ($2T_r$). The top x axis provides an estimated knot size scale based on the mean translocation velocity of each population. The majority of the knots have very short durations and thus small sizes, indicating that we are observing primarily tight knots.

As an important control, we investigated biologically knotted circular DNA plasmids that were treated with Topoisomerase IV (Topo), an enzyme that is capable of removing knots from plasmids[46]. As expected, we found that incubation with Topo led to a reduction in the number of current spikes observed (Supplementary Section 12). Circular DNA (20.7 kbp) was incubated with 4.1 μU μl^{-1} Topo for 30 min, nicked, re-purified and measured with a nanopore (4 M LiCl, 20 nm, 100 mV). Analysis of the current spikes that correspond to simple knots ($2I_1$) revealed a decrease of 31–37% in the number of events that contain these spikes for the Topo-incubated DNA relative to the controls. Because the presence of DNA-bound Topo proteins (which cause additional high-current spikes, see the Supplementary Information) counteracts the unknotting effects of Topo, this number represents a lower-bound estimate for the unknotting activity of Topo in our experimental conditions. This assay provides further and compelling evidence that the current spikes are due to knots, and shows that it is possible to assess enzymatic unknotting with this approach.

We have demonstrated that it is possible to detect knots in DNA molecules with solid-state nanopores and we have used this approach to estimate the knotting occurrence for a variety of DNA molecules with lengths far longer than previously possible. The single-molecule nature of the technique allows us to observe and analyse individual knots while still being able to generate population statistics. The measurements reveal that knots are capable of slipping out of linear molecules during translocation at a high driving voltage, so care must be taken when comparing the observed knotting rates with those predicted for molecules at equilibrium. Additionally, the knot translocation duration can be used to estimate the knot size, which is observed to be less than 100 nm for the majority of knots, although a further understanding of the translocation process is required to accurately relate this to the equilibrium knot size. From a nanopore applications perspective, efforts to sequence or detect DNA-bound proteins with nanopores will have to take into account the presence and effects of these knots[47]. These results present a major step towards the ability to directly interrogate polymer knots and thus increase our understanding of this ubiquitous phenomenon.

Methods

Methods and any associated references are available in the online version of the paper.

Received 6 October 2014; accepted 14 July 2016; published online 15 August 2016

References

1. Sumners, D. W. & Whittington, S. G. Knots in self-avoiding walks. *J. Phys. A* **21,** 1689–1694 (1988).
2. Kawauchi, A. *Survey on Knot Theory* (Springer, 1996).
3. Meluzzi, D., Smith, D. E. & Arya, G. Biophysics of knotting. *Annu. Rev. Biophys.* **39,** 349–366 (2010).
4. Staczek, P. & Higgins, N. P. Gyrase and Topo IV modulate chromosome domain size *in vivo*. *Mol. Microbiol.* **29,** 1435–1448 (1998).
5. Rodríguez-Campos, A. DNA knotting abolishes *in vitro* chromatin assembly. *J. Biol. Chem.* **271,** 14150–14155 (1996).
6. Portugal, J. & Rodríguez-Campos, A. T7 RNA polymerase cannot transcribe through a highly knotted DNA template. *Nucleic Acids Res.* **24,** 4890–4894 (1996).
7. Grosberg, A. Y. A few notes about polymer knots. *Polymer Sci. Ser. A* **51,** 70–79 (2009).
8. Metzler, R. *et al.* Equilibrium shapes of flat knots. *Phys. Rev. Lett.* **88,** 188101 (2002).
9. Orlandini, E., Stella, A. L. & Vanderzande, C. The size of knots in polymers. *Phys. Biol.* **6,** 025012 (2009).
10. Grosberg, A. Y. & Rabin, Y. Metastable tight knots in a wormlike polymer. *Phys. Rev. Lett.* **99,** 217801 (2007).
11. Tang, J., Du, N. & Doyle, P. S. Compression and self-entanglement of single DNA molecules under uniform electric field. *Proc. Natl Acad. Sci. USA* **108,** 16153–16158 (2011).
12. Bao, X. R., Lee, H. J. & Quake, S. R. Behavior of complex knots in single DNA molecules. *Phys. Rev. Lett.* **91,** 265506 (2003).
13. Arai, Y. *et al.* Tying a molecular knot with optical tweezers. *Nature* **399,** 446–448 (1999).
14. Krasnow, M. A. *et al.* Determination of the absolute handedness of knots and catenanes of DNA. *Nature* **304,** 559–560 (1983).
15. Liu, L. F., Davis, J. L. & Calendar, R. Novel topologically knotted DNA from bacteriophage P4 capsids: studies with DNA topoisomerases. *Nucleic Acids Res.* **9,** 3979–3989 (1981).
16. Trigueros, S. *et al.* Novel display of knotted DNA molecules by two-dimensional gel electrophoresis. *Nucleic Acids Res.* **29,** e67–e67 (2001).
17. Wasserman, S. A., Dungan, J. M. & Cozzarelli, N. R. Discovery of a predicted DNA knot substantiates a model for site-specific recombination. *Science* **229,** 171–174 (1985).
18. Rybenkov, V. V., Cozzarelli, N. R. & Vologodskii, A. V. Probability of DNA knotting and the effective diameter of the DNA double helix. *Proc. Natl Acad. Sci. USA* **90,** 5307–5311 (1993).
19. Shaw, S. Y. & Wang, J. C. Knotting of a DNA chain during ring closure. *Science* **260,** 533–536 (1993).
20. Ercolini, E. *et al.* Fractal dimension and localization of DNA knots. *Phys. Rev. Lett.* **98,** 058102 (2007).
21. Wasserman, S. A. & Cozzarelli, N. R. Biochemical topology: applications to DNA recombination and replication. *Science* **232,** 951–960 (1986).
22. Haque, F. *et al.* Solid-state and biological nanopore for real-time sensing of single chemical and sequencing of DNA. *Nano Today* **8,** 56–74 (2013).
23. Wanunu, M. Nanopores: a journey towards DNA sequencing. *Phys. Life Rev.* **9,** 125–158 (2012).
24. Muthukumar, M. Mechanism of DNA transport through pores. *Annu. Rev. Biophys. Biomol. Struct.* **36,** 435–450 (2007).
25. Storm, A. J. *et al.* Fast DNA translocation through a solid-state nanopore. *Nano Lett.* **5,** 1193–1197 (2005).
26. Plesa, C., Cornelissen, L., Tuijtel, M. W. & Dekker, C. Non-equilibrium folding of individual DNA molecules recaptured up to 1000 times in a solid state nanopore. *Nanotechnology* **24,** 475101 (2013).
27. Gershow, M. & Golovchenko, J. A. Recapturing and trapping single molecules with a solid-state nanopore. *Nature Nanotech.* **2,** 775–779 (2007).
28. Mihovilovic, M., Hagerty, N. & Stein, D. Statistics of DNA capture by a solid-state nanopore. *Phys. Rev. Lett.* **110,** 028102 (2013).
29. Kantor, Y. & Kardar, M. Anomalous dynamics of forced translocation. *Phys. Rev. E* **69,** 021806 (2004).
30. Rosa, A., Di Ventra, M. & Micheletti, C. Topological jamming of spontaneously knotted polyelectrolyte chains driven through a nanopore. *Phys. Rev. Lett.* **109,** 118301 (2012).
31. Huang, L. & Makarov, D. E. Translocation of a knotted polypeptide through a pore. *J. Chem. Phys.* **129,** 121107 (2008).
32. Suma, A., Rosa, A. & Micheletti, C. Pore translocation of knotted polymer chains: how friction depends on knot complexity. *ACS Macro Lett.* **4,** 1420–1424 (2015).
33. Rieger, F. C. & Virnau, P. A Monte Carlo study of knots in long double-stranded DNA chains. *PLoS Comput. Biol.* http://dx.doi.org/10.1371/journal.pcbi.1005029 (2016).
34. Ando, G., Hyun, C., Li, J. & Mitsui, T. Directly observing the motion of DNA molecules near solid-state nanopores. *ACS Nano* **6,** 10090–10097 (2012).
35. Deguchi, T. & Tsurusaki, K. A statistical study of random knotting using the Vassiliev invariants. *J. Knot Theor. Ramif.* **03,** 321–353 (1994).
36. Kowalczyk, S. W., Wells, D. B., Aksimentiev, A. & Dekker, C. Slowing down DNA translocation through a nanopore in lithium chloride. *Nano Lett.* **12,** 1038–1044 (2012).
37. Vologodskii, A. Brownian dynamics simulation of knot diffusion along a stretched DNA molecule. *Biophys. J.* **90,** 1594–1597 (2006).
38. Wang, J. C. & Davidson, N. Thermodynamic and kinetic studies on the interconversion between the linear and circular forms of phage lambda DNA. *J. Mol. Biol.* **15,** 111–123 (1966).
39. Carlsen, A. T. *et al.* Interpreting the conductance blockades of DNA translocations through solid-state nanopores. *ACS Nano* **8,** 4754–4760 (2014).
40. Rosenstein, J. K. *et al.* Integrated nanopore sensing platform with sub-microsecond temporal resolution. *Nature Methods* **9,** 487–492 (2012).
41. Kowalczyk, S. W. & Dekker, C. Measurement of the docking time of a DNA molecule onto a solid-state nanopore. *Nano Lett.* **12,** 4159–4163 (2012).
42. Plesa, C. *et al.* Velocity of DNA during translocation through a solid state nanopore. *Nano Lett.* **15,** 732–737 (2015).
43. Lu, B., Albertorio, F., Hoogerheide, D. P. & Golovchenko, J. A. Origins and consequences of velocity fluctuations during DNA passage through a nanopore. *Biophys. J.* **101,** 70–79 (2011).
44. Dai, L., Renner, C. B. & Doyle, P. S. Metastable tight knots in semiflexible chains. *Macromolecules* **47,** 6135–6140 (2014).
45. Plesa, C. *et al.* Fast translocation of proteins through solid state nanopores. *Nano Lett.* **13,** 658–663 (2013).
46. Deibler, R. W., Rahmati, S. & Zechiedrich, E. L. Topoisomerase IV, alone, unknots DNA in *E. coli*. *Genes Dev.* **15,** 748–761 (2001).
47. Plesa, C., Ruitenberg, J. W., Witteveen, M. J. & Dekker, C. Detection of individual proteins bound along DNA using solid-state nanopores. *Nano Lett.* **15,** 3153–3158 (2015).

Acknowledgements

The authors would like to thank C. Micheletti, M. Di Stefano and P. Virnau for discussions, M.-Y. Wu for TEM drilling of nanopores and R. Joseph and S. W. Kowalczyk for early experiments. This work was supported by the Netherlands Organisation for Scientific Research (NWO/OCW), as part of the Frontiers of Nanoscience program, and by the European Research Council under research grant NanoforBio (no. 247072) and SynDiv (no. 669598), the Koninklijke Nederlandse Akademie van Wetenschappen (KNAW) Academy Assistants Program and by the Wenner-Gren Foundations. Y.R. and A.Y.G. would like to acknowledge support from the US–Israel Binational Science foundation.

Author contributions

C.P., D.V., S.P., J.v.d.T., J.W.R, M.J.W. and M.P.J. carried out the measurements; C.P. and D.V. analysed experimental data; A.Y.G. and Y.R. provided theoretical interpretation; all authors discussed and interpreted results; C.P. and C.D. wrote the manuscript with input from all authors.

Additional information

Supplementary information is available in the online version of the paper. Reprints and permissions information is available online at www.nature.com/reprints. Correspondence and requests for materials should be addressed to C.D.

Competing financial interests

The authors declare no competing financial interests.

Methods

Solid-state nanopores were fabricated and used as described previously[48]. All buffers were pH 8 with 10 mM Tris and 1 mM ethylenediaminetetraacetic acid. Data analysis was carried out using Matlab scripts described in detail elsewhere[49]. Lambda phage DNA and T4 GT7 DNA were purchased from Promega (Madison, Wisconsin) and Nippon Gene (Toyama, Japan), respectively. A 20.7 kbp plasmid was grown in XL10-Gold *Escherichia coli* cells and midipreped. This plasmid was subsequently either linearized with BamHI or relaxed using the nt.BbvCI nickase. The resulting products where purified with phenol/chloroform and concentrated using ethanol precipitation. Mixed populations of both linear and circular lambda DNA were formed by heating the DNA in 2 M LiCl to 65 °C for 5 min and then placing the solution on ice until measuring. The linear 2,686 bp DNA molecules were pUC19 plasmids minipreped from *E. coli* cells and linearized with XmnI. Further methods can be found in the Supplementary Information.

References

48. Janssen, X. J. A. *et al.* Rapid manufacturing of low-noise membranes for nanopore sensors by *trans*-chip illumination lithography. *Nanotechnology* **23,** 475302 (2012).
49. Plesa, C. & Dekker, C. Data analysis methods for solid-state nanopores. *Nanotechnology* **26,** 084003 (2015).